Journal of Physiology (1992), **453**, *pp.* 663–687
With 11 *figures*
Printed in Great Britain

SYNAPTICALLY TRIGGERED ACTION POTENTIALS BEGIN AS A DEPOLARIZING RAMP IN RAT HIPPOCAMPAL NEURONES *IN VITRO*

BY G.-Y. HU*, Ø. HVALBY, J.-C. LACAILLE†, B. PIERCEY, T. ØSTBERG AND P. ANDERSEN‡

From the Institute of Neurophysiology, University of Oslo, PO Box 1104, Blindern, 0317 Oslo 3, Norway

(*Received 19 September 1991*)

SUMMARY

1. During just-suprathreshold synaptic activation of CA1 pyramidal cells in rat hippocampal slices *in vitro* the action potential begins as a slow depolarizing ramp, superimposed on the underlying EPSP and forming an integral part of the action potential. We call this ramp a synaptic prepotential (SyPP).

2. In order to examine the SyPP, a procedure for subtraction of the underlying EPSP was necessary. Because action potentials were only elicited by a subset of EPSPs with larger than average amplitude, a subtraction of the mean subthreshold EPSP would not give valid results. Instead, an EPSP to be subtracted was selected from an assemblage of subthreshold EPSPs, so that its amplitude matched the initial part of the spike-generating EPSP.

3. Virtually all action potentials started with a SyPP. Using an amplitude criterion of 1 S.D. of the mean of the matching subthreshold EPSPs, just-suprathreshold EPSPs gave prepotentials in 72–100% of all action potentials from fifteen randomly selected cells. With a criterion of 2 S.D.s, the frequency of occurrence ranged from 36 to 100%.

4. With a constant stimulus strength, there was a certain variability of the spike latencies. Shorter latency spikes had steeper, but smaller SyPPs than later spikes, suggesting that the slope of SyPP influenced the timing of the cell discharge.

5. The SyPP was best fitted by a single, exponentially rising curve, and was both smaller and slower than the large amplitude action potential. Its amplitude was 1–6 mV and the time constant 1–5 ms, which was 10–50 times slower than that of the upstroke of the action potential.

6. A properly timed hyperpolarizing current pulse could block the large amplitude action potential, thereby unmasking the SyPP as an initial depolarizing ramp.

7. The SyPP was more sensitive than the large amplitude action potential to intracellular injection of QX-314, a lidocaine derivative. At the concentrations used

* Present address: Shanghai Institute of Materia Medica, Chinese Academy of Sciences, Shanghai 200031, China.

† Present address: Département de Physiologie, Centre de Recherche en Sciences Neurologiques, Faculté de Médecine, Université de Montréal, Montréal, Québec, Canada H3C 3J7.

‡ To whom correspondence should be addressed.

MS 9783
22

(10 or 30 mM) no detectable changes were seen in the large amplitude action potential.

8. Droplet application of a specific *N*-methyl-D-aspartate receptor antagonist, DL-2-amino-5-phosphonovaleric acid (1 mM), reduced both the EPSP and the firing probability, but did not change the SyPP.

9. The SyPP amplitude and time course depended upon the membrane potential at which the cell was activated. Depolarization enhanced and prolonged the SyPP, while hyperpolarization gave opposite effects. In part, the depolarization-induced amplitude increase could be attributed to membrane accommodation.

10. Antidromically evoked action potentials never started with a prepotential. Injection of a depolarizing current pulse (5 ms) in the soma with a rising phase similar to that of the suprathreshold EPSPs gave action potentials without an initial prepotential. Longer depolarizing pulses, however, elicited action potentials starting with a prepotential.

11. The SyPPs elicited by just-suprathreshold proximal and distal inputs in the apical dendrites were nearly identical.

12. The results suggest that synaptically triggered action potentials in CA1 pyramidal cells have two phases: a slow initial prepotential followed by a fast, large amplitude action potential which are differentially sensitive to QX-314.

INTRODUCTION

Although it is often said that an excitatory postsynaptic potential (EPSP) triggers an action potential as soon as the EPSP amplitude reaches a certain voltage threshold, the classical work of Coombs, Eccles & Fatt (1955) pointed out that the relations may be more complicated. In many central nerve cells the action potential latency may vary considerably in spite of a relatively constant EPSP amplitude. In motoneurones, as for most nerve cells, action potentials are hardly ever seen to start at the peak of the EPSP as predicted by the voltage threshold idea, but at some point on the rising phase. In addition, the onset of the action potential may be difficult to determine because of the lack of an abrupt initiation (Coombs *et al.* 1955; Andersen, Storm & Wheal, 1987). In cat sensorimotor cortical pyramidal cells, Stafstrom, Schwindt, Chubb & Crill (1985) noted that an EPSP could trigger a depolarizing ramp which led to an action potential, and that hyperpolarization prevented both the ramp and the associated spike.

Based upon cross-correlograms between pre- and postsynaptic motoneuronal discharges, Knox & Poppele (1977) maintained that the temporal derivative of the EPSP gave a better definition of the action potential threshold. Other investigators have found that mixed terms of voltage and the temporal derivative of voltage fitted their data best (Kirkwood & Sears, 1982; Fetz & Gustafsson, 1983).

We now report that a process similar to the 'creep' described by Coombs *et al.* (1955) initiates synaptically triggered action potentials in rat hippocampal CA1 pyramidal cells. We have observed that the action potentials triggered by suprathreshold EPSPs consist of two parts: an initial, small depolarizing ramp, followed by a large amplitude action potential. We propose the term 'synaptic prepotential' (SyPP) for the depolarizing ramp, which seems to be an integral part of synaptically triggered action potentials. Preliminary notes describing some of the

results have been published (Andersen, Lacaille, Hvalby, Hu, Piercey & Østberg, 1986; Østberg, Hu, Hvalby, Piercey & Andersen, 1986; Hu, Hvalby, Piercey & Andersen, 1989).

METHODS

Preparation

The experiments were performed on transverse hippocampal slices taken from male Wistar rats, weighing 250–300 g. After killing the animals with ether anaesthesia, the brain was rapidly taken out and kept in cold (2–4 °C) artificial cerebrospinal fluid (ACSF) for 1–2 min. The hippocampal formation was dissected out, and transverse slices (400 μm) were cut, transferred to the experimental chamber and placed on a net in the interface between ACSF and a gas mixture of 95% O_2 and 5% CO_2. The ACSF had the following composition (mM): NaCl, 124; KCl, 2; KH_2PO_4, 1·25; $CaCl_2$, 2; $MgSO_4$, 2; $NaHCO_3$, 26; glucose, 10; and was buffered with the gas mixture to give a pH of 7·4. The temperature was kept at 32–34 °C.

Stimulation and recording

Electrolytically sharpened tungsten needles were used as stimulating electrodes, and monopolar pulses, having a duration of 10–90 μs and currents from 10 to 200 μA, were delivered at 0·5 Hz from a constant-current stimulator to proximal and/or distal sites in the stratum radiatum. In order to study the prepotentials, CA1 pyramidal cells were activated synaptically with a constant stimulus strength, aiming for a constant firing probability (FP) (range 0·2–0·6). The mean FP for the whole material was 0·49. For comparison, some cells were also activated by delivering depolarizing current pulses of different durations through the intrasomatic electrode or by antidromic stimulation of the stratum alveus. In both cases the stimulus current was adjusted to evoke a single spike with a FP of around 0·5.

The intracellular recording electrodes were made from fibre-filled micropipettes and filled with 4 M-potassium acetate. The signals were amplified using a DC amplifier, and with the high frequency filter (3 dB) set at 2 kHz. The amplifier had a bridge circuit, allowing current to be injected into the cell. The responses were recorded on FM tape for further computer analysis.

Material

The results in this report are based upon an analysis of ninety-four cells which fulfilled the following criteria: a membrane potential (MP) more negative than −60 mV, an action potential amplitude (AP) larger than 85 mV measured from the resting potential, a membrane input resistance (MR) higher than 12 MΩ measured at the end of a hyperpolarizing pulse (0·5 nA, 100 ms). The mean values and S.D. were: MP, -68 ± 6 mV; AP, 95 ± 6 mV; MR, 26 ± 9 MΩ.

Analysis

The amplified signals were analog-to-digital converted at 66 kHz, and the mean of six consecutive data points was retained, giving an actual reading speed of 11 kHz. An appropriate subthreshold EPSP was subtracted from each spike-containing trace to visualize the prepotential and the following action potential. The selection of the appropriate EPSP is described in the text. The subtracted records – each containing an action potential with its initial prepotential component – were averaged with reference to the upstroke of the action potential. The form, number of components, amplitude and time course of the subtraction records were assessed by a curve-fitting program (Provencher, 1976). If not elsewhere described, data are presented as means $\pm$ S.D., and the statistical significance was calculated using Student's two-tailed t test.

Modulation

In one series of experiments, the lidocaine derivative QX-314 (Astra, Södertälje, Sweden) was injected from the intracellular electrode. The drug (10–100 mM in 4 M-potassium acetate) was delivered by 500 ms depolarizing current pulses (1–2 nA) in a 50% duty cycle for periods of 5 min. DL-2-Amino-5-phosphonovaleric acid (APV, Sigma) was applied onto the surface of the slice near the recording site through a glass pipette (1 mM, 8 nl).

RESULTS

Appearance of synaptic prepotentials

In intracellular records from CA1 pyramidal cells stimulation of afferent fibres in stratum radiatum at a given strength elicited EPSPs with or without superimposed action potentials. In the sample records in Fig. 1*A* and *B*, taken from two different cells, all action potentials begin as a short (3–5 ms) depolarizing ramp, the synaptic prepotential (SyPP). The ramp suddenly changes into the fast rising, large amplitude action potential. For each sample, the stimulus strength was kept constant. In single records such ramps are easily seen to start long latency spikes, particularly at more depolarized membrane potentials (Fig. 1*C*).

If the action potentials had taken off from the peak of the EPSPs, the threshold for their fast rising phases should be found close to the upper amplitude envelope of the subthreshold EPSPs. However, Fig. 1*C* shows that this threshold was always found at a more positive level than the largest subthreshold EPSP. Here, a large number of responses from the same cell as in *A* are presented. The constant stimulus strength straddled the threshold for action potential generation. The upper panel shows the superimposed records where the trajectory of the largest amplitude subthreshold EPSP is marked by white dots. In the lower panel all subthreshold EPSPs are shown with the thresholds for the large amplitude action potentials given by the black dots. These threshold points were identified by the computer after initial experiments had shown the transition to the upstroke of the action potential (maximal d^2V/dt^2) to occur 0·54 ms (six digitizing steps) before its highest rate of rise. The linear regression line through the threshold points (dashed line) was nearly horizontal and with a definite distance from the largest subthreshold EPSP (2·5–4·0 mV). The small standard error of the estimate (0·04 mV) indicates a strict linear regression for the threshold points, which had a mean value of −49 mV.

Action potentials are triggered by a subset of EPSPs

Subtraction of the underlying EPSP from the total response should expose the action potential with any pre- and after-potentials. However, there was an appreciable variation in the time of occurrence of the action potentials from one trace to the next. In addition, the random synaptic noise of about 0·5–2 mV peak-to-peak, required that the records were averaged to demonstrate the form of the evoked response. In order to find an acceptable EPSP waveform to subtract, we first asked whether action potentials were elicited by the whole range, or only by a subset of EPSPs. A large number of records was gathered in response to a constant stimulus strength. In Fig. 2*A*, the upper continuous line represents the averaged trace of fifty-nine responses with action potentials. The lower, continuous line gives the mean of seventy-one subthreshold EPSPs and the two dotted lines trace the largest and smallest of these EPSPs. The averaged suprathreshold synaptic potential clearly differs from the averaged subthreshold EPSP. Figure 2*B*, *C* and *D* shows amplitude histograms of the supra- and subthreshold EPSPs (filled and open bars, respectively), taken at the times indicated by the arrows labelled *b*, *c* and *d* in *A*. The *P* values show the two EPSP sets to be statistically different from an early point on the rising phase. Consequently, although the input was intended to be constant, action potentials only emerged from a subset of larger than average EPSPs. Similar histogram analyses in

twenty-one other cells gave corresponding results. Therefore, the mean subthreshold EPSP cannot be used for subtraction.

Subtraction procedure

In a search for a better trace to be used for subtraction, the main idea was to estimate the continuation of the EPSP trajectory, had an action potential not

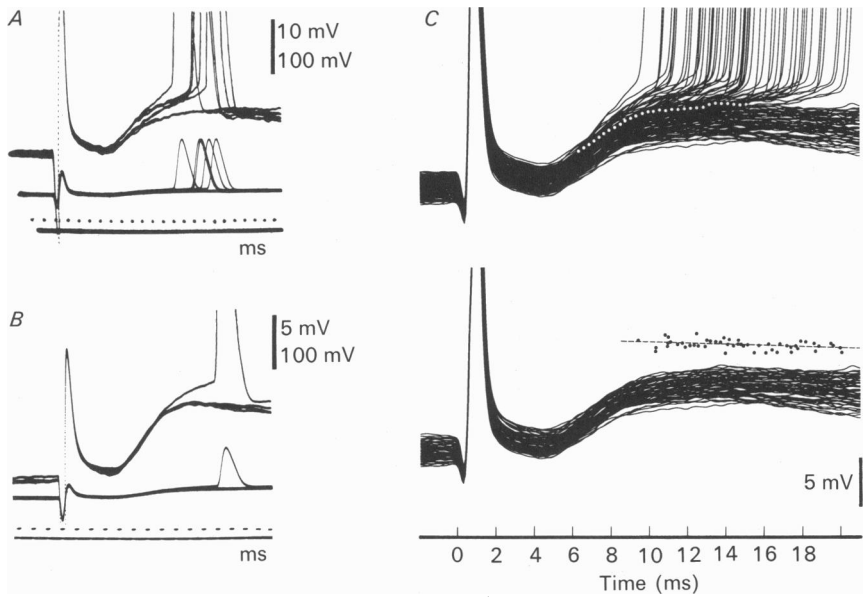

Fig. 1. Synaptically elicited action potentials in CA1 pyramidal cells. *A* and *B*, intracellular records from two cells in response to orthodromic activation at threshold strength displayed at high and low gain. Action potentials start as slow depolarizing ramps. *C*, the responses from the same cell as in *A* elicited by constant stimuli. In the upper panel fifty-nine supra- and sixty-six subthreshold responses are superimposed. The falling phases of the action potentials have been removed for clarity. The trajectory of the largest subthreshold EPSP is marked by white dots. In the lower panel only the subthreshold EPSPs and the threshold points for the large amplitude action potentials (black dots) are presented. The dashed line is the linear regression line for the points. There is a gap between these points and the largest subthreshold EPSP. The cell had a resting potential of −66 mV and was depolarized to −58 mV by current injection.

appeared. For each EPSP giving rise to an action potential another EPSP was selected from a collection of all subthreshold EPSPs elicited by the same stimulus strength, so that the initial parts of the two EPSPs matched each other in form and amplitude. The use of such templates was accepted because preliminary tests showed the various amplitude EPSPs, elicited by the same stimulus strength, to have closely congruent shapes (Fig. 3*A*). A large number of subthreshold EPSPs were divided into three groups based on their amplitude, which were averaged and labelled u, m and l, respectively. The near-constant ratios as a function of time, resulting from dividing the curve u with m and with l (dots, lower panel), demonstrate the congruence of the EPSP shapes. This also applied to the fraction of subthreshold EPSPs which was as large as the spike-generating EPSPs. The procedure also

demonstrates that isolated prepotentials are not elicited by the greater subthreshold EPSPs, because this would have given a different shape of the largest EPSPs (u) compared to the others.

In Fig. 3*B*, an example is given where the smallest and largest EPSP of a subthreshold assemblage are given by the small dots. The stretch of a single spike-

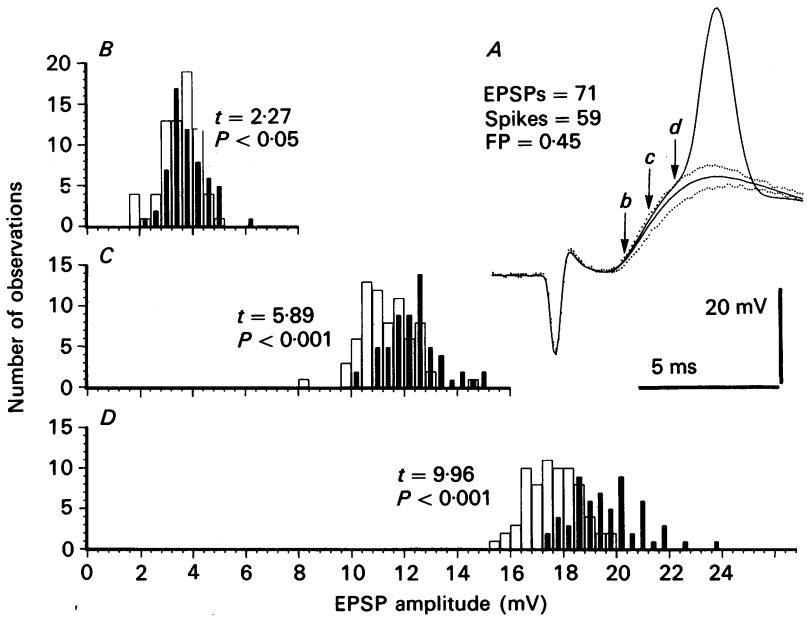

Fig. 2. Amplitude distributions of supra- and subthreshold EPSPs. *A*, the averaged supra- and subthreshold responses (the upper and lower continuous traces) of a CA1 pyramidal cell to a constant stimulus strength. The dotted lines show the largest and the smallest subthreshold EPSPs. Spikes and EPSPs, the number of the supra- and subthreshold responses. FP, the firing probability. Amplitude histograms were constructed for every 0·45 ms (five digitizing points) from the EPSP onset to the latency of the earliest large amplitude action potential for both groups of responses. *B–D*, the amplitude distributions of supra- (filled columns) and subthreshold EPSPs (open columns) at the points indicated in *A* (*b*, *c* and *d*). The *t* values (Student's test) and the corresponding *P* values are presented.

containing trace (continuous line) which was used as a template for matching is marked with two arrows. In order to reduce the effect of noise the mean value of those four EPSPs that lay closest to the spike-containing trace was used for subtraction (big dots). At the bottom of Fig. 3*B* a sample subtraction record is presented, showing that the action potential began as an initial ramp, the SyPP. The effect of template length is discussed on p. 670.

By summing a number of subtraction traces as in Fig. 3*B*, using the steepest rate of rise of the action potential as the time reference, an averaged record could be produced as shown in the following figures. In some cases, particularly for short latency spikes (earliest quartile), for which sufficiently large subthreshold EPSPs were not found, the mean of the four largest EPSPs was enlarged in proportion to fit the template.

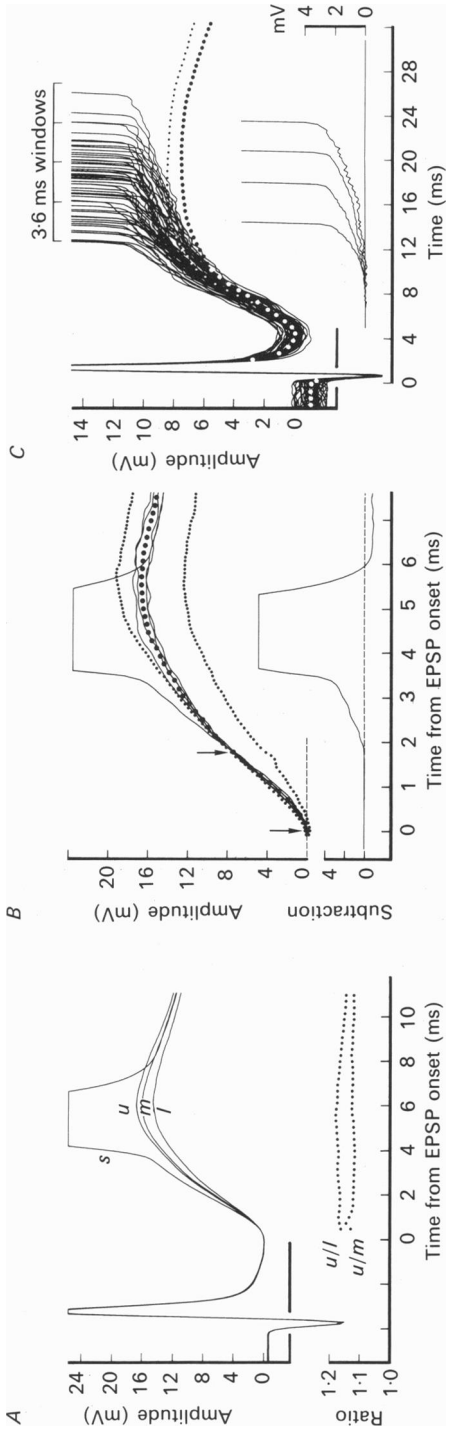

Fig. 3. Subtraction procedure and time window analysis. *A*, the mean of thirty-seven spike-containing records (trace *s*) from a CA1 pyramidal cell in response to a given stimulus strength. The traces *u*, *m* and *l* represent the mean values of three subgroups of subthreshold EPSPs (twenty-seven in each) based upon their amplitude in response to the same stimulus strength. In the lower panel the ratios of the trace *u* to trace *m* or *l* gave approximately constant values for the EPSPs, indicating congruence of shape of the various EPSPs of the sample. *B*, a single spike-containing record from the same cell (the upper continuous trace). The first half of the rising phase of this record was arbitrarily taken as the template (stretch between arrows). The small dots mark the envelope of eighty subthreshold EPSPs to the same stimulus strength. From this assemblage four subthreshold EPSPs, namely the two lying closest to the template on either side (continuous traces), were selected and the mean value (large dots) was subtracted from the original spike-containing record. The lower panel shows a subtraction record: an action potential starting as a ramp, the SyPP. *C*, another CA1 pyramidal cell responded to 135 constant stimuli with fifty-five action potentials. The mean values of eighty subthreshold EPSPs and fifty-five subthreshold EPSPs selected for subtraction are given by the large and small dots, respectively. Based upon their latency the action potentials were assigned to one of four 3·6 ms time windows. For each window the individual subtraction records were first aligned with respect to the steepest rate of rise of the action potential, then averaged, and drawn at the median spike latency for that window. As a result, four averaged SyPPs with the initial parts of the large amplitude action potential are presented in the lower panel.

Time window analysis

Within a long series of responses to a constant stimulus strength, the SyPP varied in both amplitude and duration. In general, short latency action potentials had relatively short and steep SyPPs, whereas the SyPPs of longer latency spikes were longer and larger. To obtain a better description of the SyPP, therefore, the whole range of firing latencies was divided into several equally wide time windows and an averaged SyPP was calculated for the traces belonging to each window. Figure 3*C* illustrates such an analysis for a cell in which the constant stimuli caused a FP of 0·41. Four time windows, each 3·6 ms wide, were used to divide the action potentials into groups. Within each group, the subtraction procedure was applied for each spike-containing trace. The resulting subtraction records were averaged with respect to the spike and drawn at the median spike latency of the group. The rising phase of the SyPPs was steeper the shorter the action potential latency (Fig. 3*C*, lower traces). The SyPP amplitudes were very similar for the different spike latencies (Fig. 1). Only for particularly long latencies did the SyPP amplitude increase, mostly due to the subtraction of a declining EPSP, but also because of some accommodation.

The strong correlation between the latency of the action potential and the steepness of the SyPP in a situation with a nearly constant EPSP suggests that the slope of the SyPP has an important influence on the timing of the discharge.

Twenty cells were analysed at different stimulus strengths. There was an inverse relation between the SyPP amplitude and its rise time constant on the one hand, and the FP and the EPSP size on the other. Since the SyPP is the result of a subtraction, its amplitude will go down when the EPSPs are large, as with high FP. This finding accentuates the importance of a constant FP when the effect of any manipulation on SyPPs is to be estimated.

Importance of the template length

In the subtraction procedure described above, the end of the template period was chosen arbitrarily (Fig. 3*B*). To test to what extent the position of the end-point could influence the SyPPs obtained, the duration of the template was increased progressively along the rising phase of EPSP from the onset of the EPSP towards the earliest action potential (arrows 1–6 in Fig. 4*A*). For each template duration a set of SyPPs was obtained with the subtraction procedure (Fig. 4*B*), and their amplitudes and rise time constants were plotted (Fig. 4*C*). A duration of the template comprising between about 20 and 60% of the rising phase of the EPSP (up to points 2–4) gave similar subtraction traces, particularly for the two latest time windows (Fig. 4*C*, open symbols). With the shorter templates the relatively large proportion of noise often caused the selection of inappropriate EPSPs for subtraction. Longer templates, lasting more than 60% of the rise time (templates 0–5 and 0–6), resulted in the selection of an erroneously enlarged EPSP. The reason was that a part of the SyPP was included in the template. Such conditions gave a certain underestimation of the SyPPs, particularly of those coupled to the early spikes (Fig. 4*B*). As a compromise, the first half of the EPSP rising phase was chosen as the template for all subtraction procedures.

Form and amplitude of the synaptic prepotential

The SyPP differs in shape from the EPSP. When aligned on the upstroke of the action potential, the SyPP has an upward concave form (Figs 3*C* and 4*B*), whereas the EPSP is upward convex for the major part of its rising phase. This applies to the subthreshold EPSPs of all amplitudes (Figs 1*C* and 3*A*).

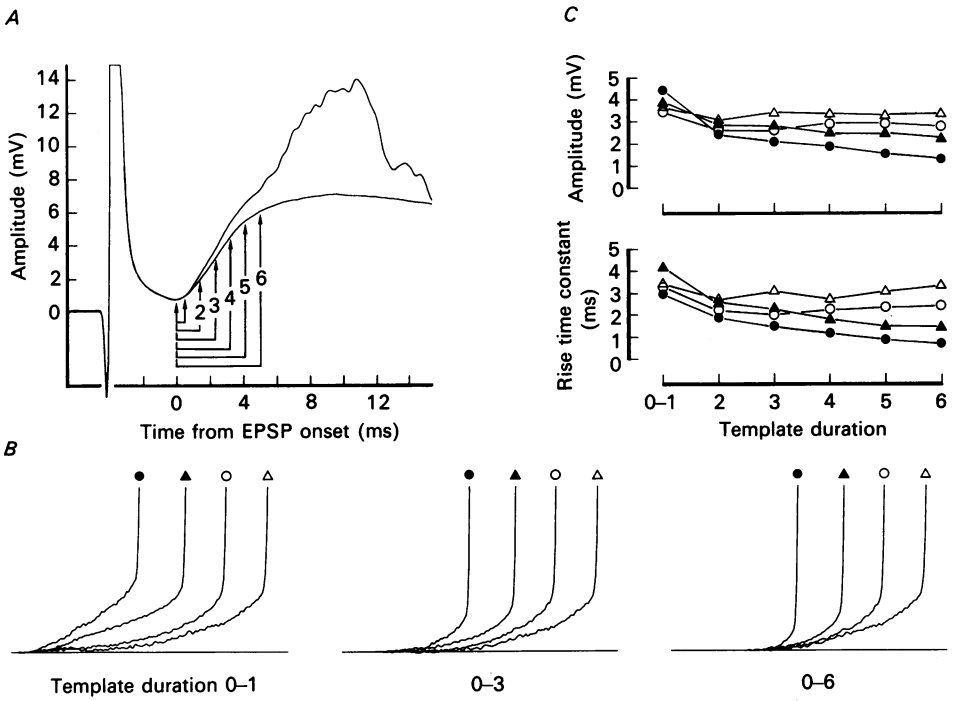

Fig. 4. The template length and the SyPP. *A*, the averaged traces of fifty-seven action potentials and sixty-eight subthreshold EPSPs from a CA1 pyramidal cell in response to constant orthodromic stimuli. The template started at the EPSP onset ($t = 0$ ms), and ended at points 1–6 along the rising phase of the EPSP, as indicated by the labelled arrows. *B*, three samples of SyPPs taken with the templates 0–1, 0–3 and 0–6, each with four time windows marked with ●, ▲, ○ and △, respectively. The voltage and time scales are the same for *A* and *B*. *C*, the amplitudes and the rise time constants of the SyPPs plotted as functions of the template duration using the same symbols as in *B*. The values in the same time windows are connected with lines.

In order to describe the form of the SyPP in more detail, a set of averaged subtraction records was first derived, using the method of time window analysis illustrated in Fig. 3*C*. Of several algorithms, including linear, hyperbolic, parabolic and exponential functions, a single exponential gave the best fit to the SyPP using the sum of least squares. The inset in Fig. 5*A* shows the averaged prepotentials from a CA1 pyramidal cell activated by a constant stimulus strength. The traces are arranged in three latency groups. Below are the records plotted on a semilogarithmic amplitude scale (●) from their start to a point representing the steepest slope of the action potential (labelled 0 ms). Exponential curves fitted to the data appear as

straight lines and the time constant of each curve is given. By subtraction of the slow component from the total data set, a fast component is revealed (○), corresponding to the fast rising phase of the action potential. This rapid component had a time constant of 0·11 ms in this cell, which was more than one order of magnitude less than

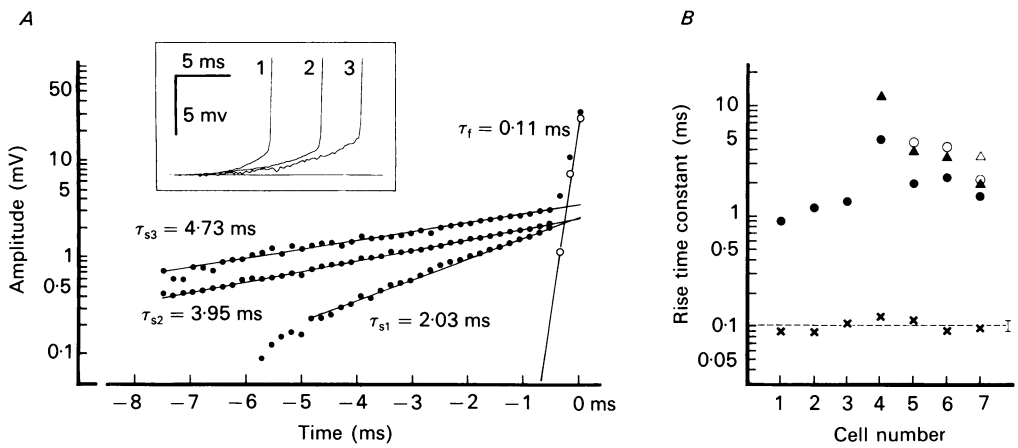

Fig. 5. Form and rise time of the SyPP and the large amplitude action potential. *A*, three averaged subtraction records obtained by using the time window analysis on fifty-five action potentials and eighty subthreshold EPSPs recorded from a CA1 pyramidal cell in response to constant stimuli (the inset). Below, the three records are plotted on a semilogarithmic amplitude scale (●) from the start to a point representing the steepest slope of the action potential (labelled 0 ms). The three gently sloping straight lines give the exponential fit for the main part of the SyPPs, starting from the first point to exceed an amplitude of 0·25 mV and ending at a point 0·54 ms before the steepest part of the action potential. The three remaining points belong to record 3 in the inset. After subtracting the slow component, the open circles show the voltages for these three values which represent the initial upstroke of the large amplitude action potential and the steep line gives the exponential fit. τ_f and τ_s, the time constants for the fast and slow components. *B*, the rise time constants for the averaged SyPP and the large amplitude action potential from seven randomly selected cells presented with a logarithmic ordinate. The crosses at the bottom give the rise time constants for the large amplitude action potential. The mean and S.D. are indicated by the dashed line and bar. Cells 1–3 had action potentials in one time window only, while cells 4–7 had them in two to four time windows. The four different symbols (●, ▲, ○ and △) represent the rise time constants of the SyPPs in the successive time windows.

those of the SyPPs, and was virtually identical for each of the three averaged large amplitude action potentials in the inset.

A regular finding was the abrupt change in the slope of the traces at the start of the upstroke of the action potential (within 0·18 ms, at −0·54 ms in Fig. 5*A*). The degree of fit was as good in the last third of the SyPP (from about −3·0 to −0·54 ms) as in its two first thirds (from about −7·6 to −3·0 ms). Taken together, the two parts of the traces (before and after −0·54 ms) appear to follow distinctly different time courses without an identifiable transition phase, suggesting the presence of two separate processes.

The large difference between the time constants for the SyPP and the large amplitude action potential is further demonstrated in Fig. 5*B*. For seven randomly selected cells the time constant for the large amplitude action potential ranged from

0·09 to 0·13 ms (×). The mean value and S.D. was 0·11 ± 0·01 ms (dashed line and bar). The filled circles give the time constant of the SyPPs which were coupled to spikes in the shortest latency window for each cell. Cells 4–7 had action potentials in several latency groups, and the various symbols indicate the time constants for the

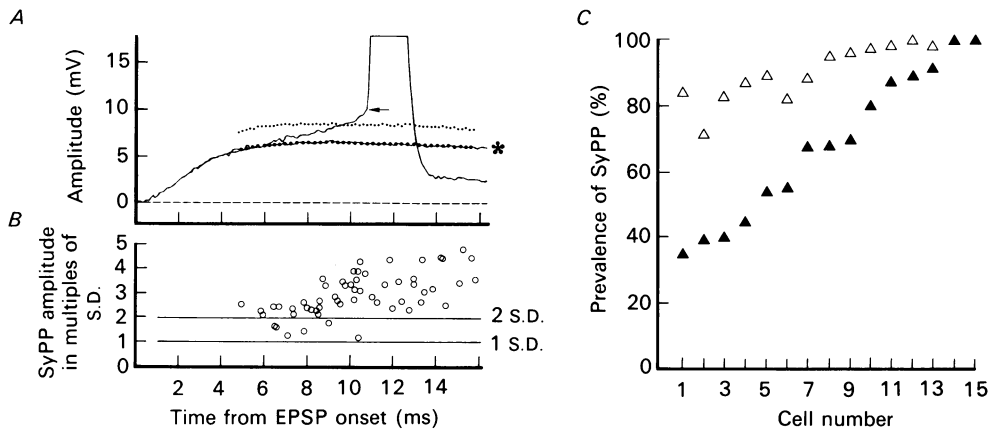

Fig. 6. Prevalence of SyPP. *A*, one of the fifty-seven spike-generating EPSPs with its best-matching subthreshold EPSP (continuous trace, asterisk) elicited by a constant stimulus strength in a CA1 pyramidal cell. The large and small dots give the mean of all fifty-seven matching subthreshold EPSPs and is the addition of 2 S.D.s to the latter, respectively. The voltage difference between the threshold of the large amplitude action potential (arrow) and the matching EPSP represents the amplitude of the SyPP and is well above the 2 S.D. level. *B*, the amplitude of SyPP coupled to each spike expressed as multiples of the standard deviation, S.D., and plotted against the spike latency. The 1 and 2 S.D. levels are indicated by two horizontal lines. *C*, the percentage of spikes with SyPP amplitudes larger than 1 (△) and 2 (▲) S.D.s of the amplitudes of all matching EPSPs from fifteen randomly selected cells. The data have been arranged in ranked order.

corresponding SyPPs. The time constant of the SyPP was between 10 and 50 times longer than that of the large amplitude action potential.

Prevalence of the synaptic prepotential

With appropriate conditions for detection, we observed SyPPs in nearly all cells in the present material (92/94). However, in individual sweeps random synaptic noise and other spontaneous fluctuations tended to mask the SyPPs. In order to obtain an estimate of the degree of coupling between the SyPP and the large amplitude action potential, we analysed all action potentials triggered by constant stimulus strength in fifteen randomly selected cells. Preliminary investigations showed that the large amplitude action potential started 0·45–0·54 ms before the maximal dV/dt (Fig. 5*A*). The amplitude of SyPP was taken as the voltage difference between the threshold of the large amplitude action potential (indicated by arrow in Fig. 6*A*) and the matching subthreshold EPSP (thin line under the large dots, asterisk). The amplitude of the SyPP was expressed in multiples of the S.D. of the mean selected EPSP amplitude at the same point (Fig. 6*B*). For the cell shown in Fig. 6*A* most SyPPs had an amplitude greater than 2 S.D.s of the mean selected EPSP. Typically, the amplitudes were larger for the later spikes to a given stimulus strength. In Fig. 6*C* the percentages of spikes with SyPP amplitudes larger than 1

(△) and 2 S.D.s (▲) of the mean selected EPSP amplitude are plotted in ranked order for the same fifteen cells. On the 1 S.D. criterion, the cells showed a frequency of SyPP occurrence of 91% (range 72–100%), and 70% (range 36–100%) on a 2 S.D. criterion. The strong coupling between the SyPP and the large amplitude action potential suggests that the SyPP normally evolves into, or triggers, the latter.

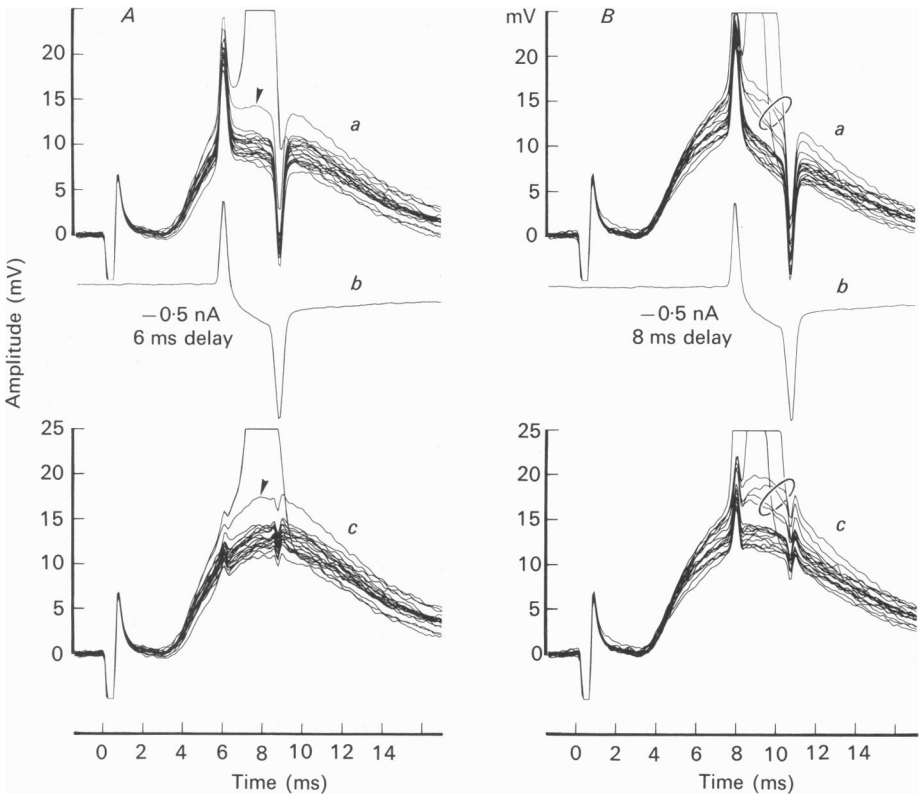

Fig. 7. Unmasking of SyPPs. *A*, the synaptic responses of a CA1 pyramidal cell to a constant stimulus strength superimposed by short hyperpolarizing current pulses (3 ms, −0·5 nA) with a delay of 6 ms (upper panel). The traces in the lower panel (*c*) are the computer subtractions of the averaged isolated pulse response (*b*) from the superimposed responses (*a*). The arrow-head indicates a trace, which failed to lead to firing, but with a considerably larger amplitude than the other subthreshold EPSPs. *B*, as *A*, but with a pulse delay of 8 ms. Two of the six highest amplitude traces (encircled) gave rise to action potentials; the other four traces, which failed to discharge, had amplitudes 2–7 mV above the subthreshold EPSPs. In *B* four short latency (< 7·5 ms) action potentials have been omitted for clarity.

Isolation of the synaptic prepotential

We attempted to block the large amplitude action potential by injecting a short hyperpolarizing pulse. This was timed to occur during the developing SyPP, and just before the expected appearance of the large amplitude action potential (Fig. 7). Without any hyperpolarizing pulses, the illustrated cell had a FP of 0·37. When properly timed, the pulse prevented most spike discharges. The top panels show the

synaptic responses with superimposed current pulses. The middle traces show the averaged hyperpolarizing pulses and below the subtraction traces are displayed. In *A*, two of the eighteen traces had a particularly large amplitude just before the pulse artifact. One of these traces continued as an action potential, whereas the other

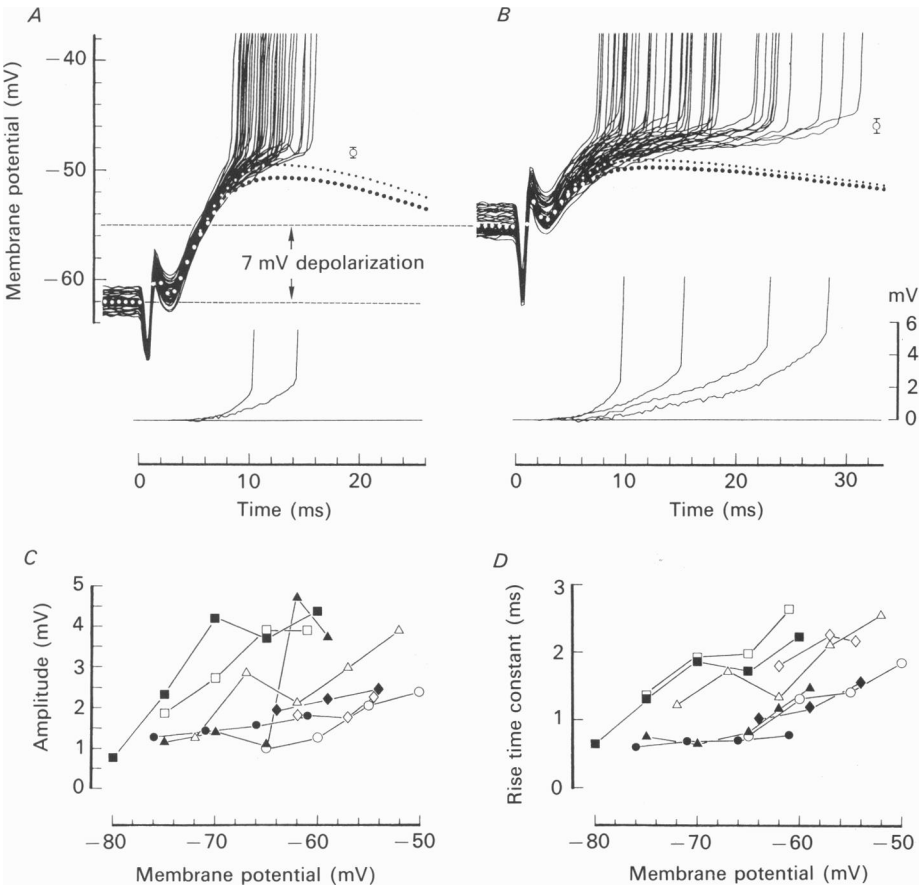

Fig. 8. Effect of depolarization on the SyPPs. *A*, this CA1 cell responded to a series of 107 constant stimuli (32 μA) with forty-eight action potentials at a membrane potential of −62 mV (upper panel). The mean of fifty-nine subthreshold EPSPs and the mean of forty-eight subthreshold EPSPs selected for subtraction are given by the large and small dots, respectively. The mean of the thresholds for the large amplitude action potentials is given by the open circle and bar. *B*, at −55 mV the same cell responded to a reduced stimulation strength (29 μA) with fifty-three action potentials and forty subthreshold EPSPs. The large amplitude action potentials occurred with more variable latencies at a higher threshold. In both cases time windows of 6 ms were used for the subtraction procedure. *C* and *D*, the amplitudes and rise time constants of the SyPPs from eight randomly selected CA1 cells plotted against the membrane potential. Different symbols give values from different cells in the first time window (6 ms), tested at three to five membrane potential levels.

remained considerably higher than the rest of the traces (arrow-head). The rest of the traces had the sample amplitude distribution as control subthreshold EPSPs. In *B*, the pulse delay was increased from 6 to 8 ms, giving longer time for the SyPP to develop. Here, there were six large amplitude records (encircled) out of a total of eighteen, of which two gave rise to action potentials. The four remaining traces appeared as smooth waves with amplitudes 2·5–6·0 mV above the largest subthreshold EPSP. These traces derived from the same upper range of EPSPs that normally elicit action potentials. They also appeared with roughly the same probability (0·45) as spikes did when no blocking pulse was applied. Statistically, the amplitudes of the encircled traces in Fig. 7*B*, measured 1 ms before the pulse, are unlikely to be drawn from the same sample as the subthreshold EPSPs ($P < 0·01$). Therefore, we conclude that the labelled large amplitude traces in Fig. 7*A* and *B* probably represent isolated SyPPs which were prevented from generating spikes by the hyperpolarizing pulses. Similar results were seen in the three other CA1 pyramidal cells tested. In two of them, progressive increase of the amplitude of the hyperpolarizing pulse caused increased delay of the action potential coupled to a prolonged duration of the associated SyPPs (not shown).

Effect on the synaptic prepotential of membrane potential changes

Both the amplitude and the rise time course of the SyPP depended upon the membrane potential. In Fig. 8*A*, the cell responded with a FP of 0·45 at a membrane potential of −62 mV, and the large amplitude action potentials took off at a threshold of $-48·3 \pm 0·5$ mV (open circle and bar), well above the trajectory of the mean of the EPSPs selected for subtraction (small dots). After the cell was depolarized 7 mV by injection of a steady current through the recording electrode, the scatter of the spike latencies increased greatly in response to a reduced stimulation strength to keep a comparable FP, a phenomenon we found regularly (Fig. 8*B*). The SyPPs (below) increased in amplitude, particularly for the longer latencies. A major part of this change may be explained by an elevated spike threshold which now measured $-45·9 \pm 0·7$ mV. Typically, the SyPPs associated with the longer latency spikes had a considerably slower time course than the earlier ones.

The same type of changes were seen in all thirty-eight CA1 pyramidal cells tested at three to five membrane potential levels. In Fig. 8*C* and *D* the SyPP amplitude and rise time constant from eight randomly selected cells were plotted as functions of membrane potential. For clarity, only data for the SyPPs coupled to the short latency spikes within the first time window of 6 ms are presented. In spite of the variability from one cell to the next, the results from all cells show the same tendency. A linear regression estimate through all data points in Fig. 8*C* and *D* indicates that there is a weak, positive correlation between the size of the SyPP and the membrane potential level. Due to the scatter between the data from individual cells the correlation coefficient was only 0·37, but statistically significant ($P < 0·05$). The rise time constant of the SyPP was more clearly correlated to the membrane potential, with a correlation coefficient of 0·56 ($P < 0·01$). Thus, depolarization towards the firing level for the action potential increased both the amplitude and the rise time constant of the SyPP.

Pharmacological manipulations of the synaptic prepotential

Injection of QX-314 (100 mM) from the intracellular recording microelectrode blocked the SyPP within 2–5 min, and there was also a reduction of the large amplitude action potential. With lower concentrations (10 or 30 mM) it was possible to selectively block the SyPP. Within tens of minutes the SyPP was gradually reduced in twenty-three cells and completely blocked in five of them. The reason for the failure to achieve full blockade in most cells may have been that they were lost before sufficient amounts of the drug had been ejected.

Results from a representative experiment are illustrated in Fig. 9*A–C*. Before the injection of QX-314, an orthodromic stimulus of 103 μA gave the CA1 cell a discharge probability of 0·41. A set of averaged subtraction records obtained by the time window analysis is presented underneath (Fig. 9*A*). After injection of QX-314, the same stimulus strength failed to discharge the cell (FP = 0). The cell did fire to stronger stimuli (Fig. 9*B*), but the action potential was now preceded by a tiny ramp only, most of which can be attributed to a stronger extracellular field potential (uneven EPSP shape) that is associated with stronger stimuli. In contrast to the nearly total block of the SyPP, the large amplitude action potential showed no detectable change in amplitude (Fig. 9*C*). Therefore, after the QX-314 injection had removed the SyPP, a larger EPSP was needed to elicit the action potential.

An alternative explanation of the SyPP blockade is a suppression of the underlying EPSP to a value below the SyPP threshold. Therefore, the effect of QX-314 on the EPSP was analysed in seven CA1 cells. During a total of twelve injections of QX-314 the SyPPs were gradually reduced to a level between 45 and 0% of the original value, while the ratio between the averaged peak EPSP amplitude before and after the injection was unchanged ($1{\cdot}02 \pm 0{\cdot}15$, not significant, Student's paired t test). The declining phase of the EPSP was also unchanged. The effect of QX-314 on the membrane potential was examined in thirteen of the twenty-three cells. QX-314 injected in a total of twenty-six sessions tended to depolarize the cells slightly ($2{\cdot}3 \pm 3{\cdot}9$ mV, $P < 0{\cdot}01$). However, a depolarization of this magnitude should by itself enhance, rather than depress, the SyPP.

Several lines of evidence suggest a NMDA receptor-mediated component in normal synaptic transmission in hippocampal CA1 pyramidal cells (Hablitz & Langmoen, 1986; Andreasen, Lambert & Jensen, 1989). The NMDA receptor-mediated component increases with depolarization and thus behaves similarly to the SyPP. As shown in Fig. 9*D–F*, droplet application of D-aminophosphonovalerate (APV), a specific NMDA receptor antagonist, did not change the SyPP, although a transient reduction of the FP and the EPSP, particularly its falling phase, appeared 5 min after the application. Similar results were seen in two other cells tested.

Short depolarizing pulses and antidromic activation elicited action potentials without prepotentials

Since a just-suprathreshold EPSP regularly produced SyPPs, we examined whether a similarly short depolarizing current pulse delivered to the soma membrane could do the same. Consequently, we delivered pulses of 5 ms duration to match the rise time of the EPSP and adjusted the injected current to give a FP of around 0·5.

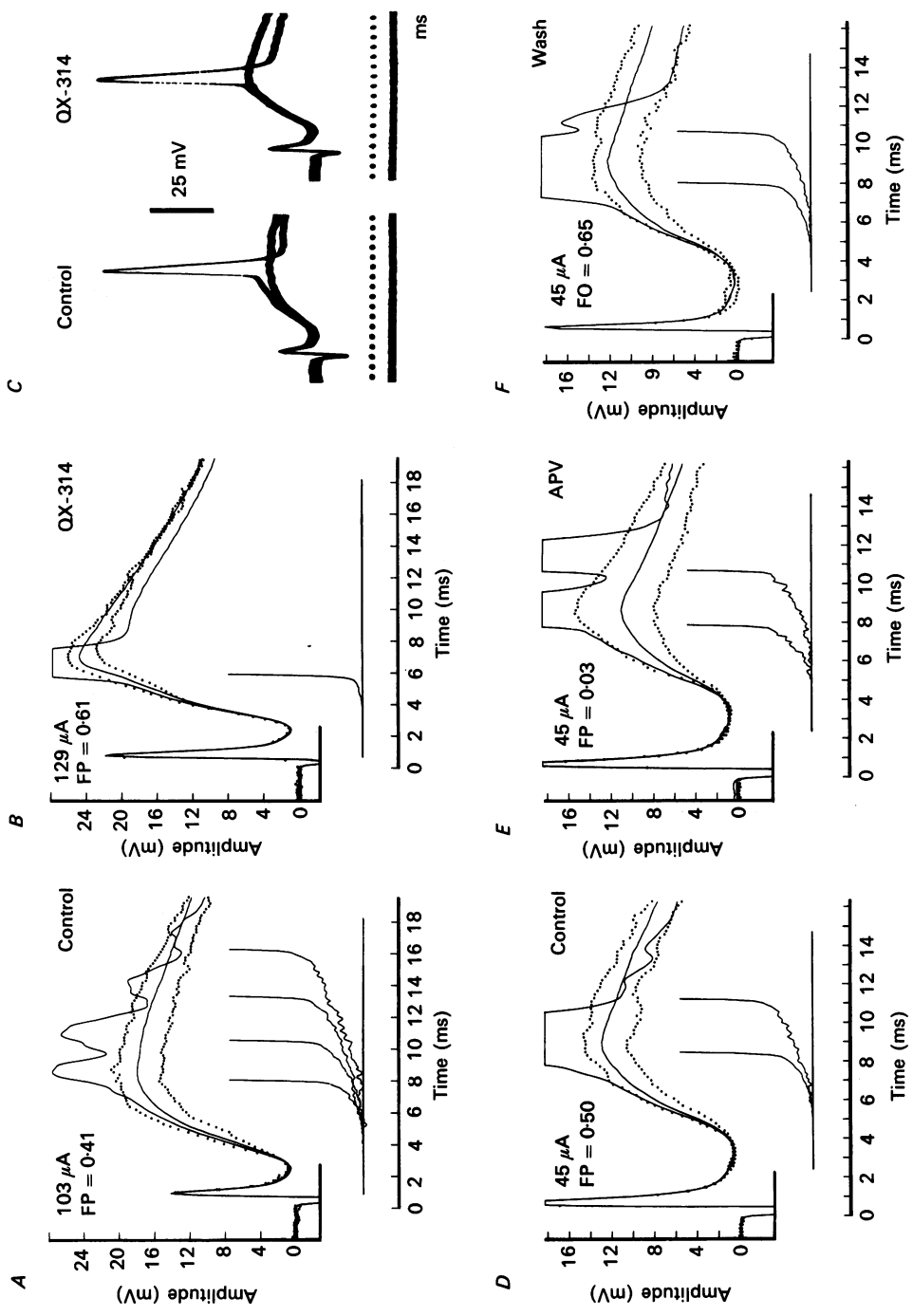

Fig. 9. For legend see facing page.

In eighteen cells in which a full analysis was made, we never observed any prepotential preceding the action potential (Fig. 10*B*). All cells showed, however, clear prepotentials to synaptic activation (Fig. 10*A*) and to longer pulses (Fig. 10*C*).

Figure 10*D–H* shows the averaged subtraction records from the same cell in response to pulses of 5, 10, 20, 40 and 80 ms duration, drawn to the same time scale. In each case, the depolarizing current was adjusted to evoke a single spike with a FP of around 0·5. Only the longer pulses gave slow prepotentials. The slow prepotential to 10 ms duration pulses is either absent or just discernible, while the 5 ms pulses did not give rise to any prepotential at all. With increasing pulse duration the threshold for the action potential moved in a positive direction, being largely responsible for the increased amplitude and duration of the pulse-induced slow prepotentials.

Antidromic invasion by stimulating the stratum alveus was also unable to create any prepotential although it efficiently drove the cell to discharge as tested in twelve CA1 pyramidal cells (not shown). The failure of a short depolarizing pulse or antidromic activation to elicit a prepotential suggests that the soma and the initial segment are unlikely generation sites for prepotentials.

Synaptic prepotentials elicited by proximal and distal inputs

Stimulation of afferent fibres making synapses at various levels of the central 4/5ths of the dendritic tree has been shown to be able to produce SyPPs. A possible large SyPP amplitude associated with a distal dendritic EPSP position could conceivably explain the unexpectedly high efficiency of peripheral synapses as compared with proximal ones (Andersen, Silfvenius, Sundberg & Sveen, 1980). For this reason, we compared the size of the SyPPs produced by equally effective proximal and distal synaptic stimulation to the same cell. In a group of eight cells with well-matched FP for both inputs (FP difference less than 0·05 and tested at a total of twelve different membrane potential levels) no statistically significant differences in the amplitude or the rise time were found for the SyPPs produced by distal and proximal inputs. In the example shown in Fig. 11*A* and *B* the mean subthreshold EPSP (large dots) and the mean of the EPSPs selected for subtraction

Fig. 9. The SyPP is sensitive to QX-314 injection, but not to APV application. *A*, the averaged traces of twenty-six action potentials and thirty-seven subthreshold EPSPs (continuous traces) from a CA1 pyramidal cell in response to a constant stimulus strength before QX-314 injection. The largest and smallest subthreshold EPSPs are given by the dots. The averaged subtraction records are shown at the bottom. *B*, the averaged traces of twenty-five action potentials and sixteen subthreshold EPSPs in response to an increased stimulus strength after injection of QX-314 (10 mM, 175 nC). The averaged subtraction record shows a tiny ramp in front of the upstroke of the large amplitude action potential. *C*, the superimposed records with and without an action potential from the same cell before and after QX-314 injection displayed at low gain. *D*, the averaged traces of forty-five action potentials and forty-six subthreshold EPSPs from another cell before APV application. *E*, the averaged traces of two action potentials and seventy-eight subthreshold EPSPs recorded 5–8 min after a drop of APV solution (1 mM, 8 nl) was applied near the recording site on the surface of the slice. *F*, the averaged traces of forty-three action potentials and twenty-three subthreshold EPSPs 30 min after the APV application. The stimulus strength was kept constant throughout the experiment. Same voltage scale for the upper and lower panels in *A*, *B*, *D*, *E* and *F*.

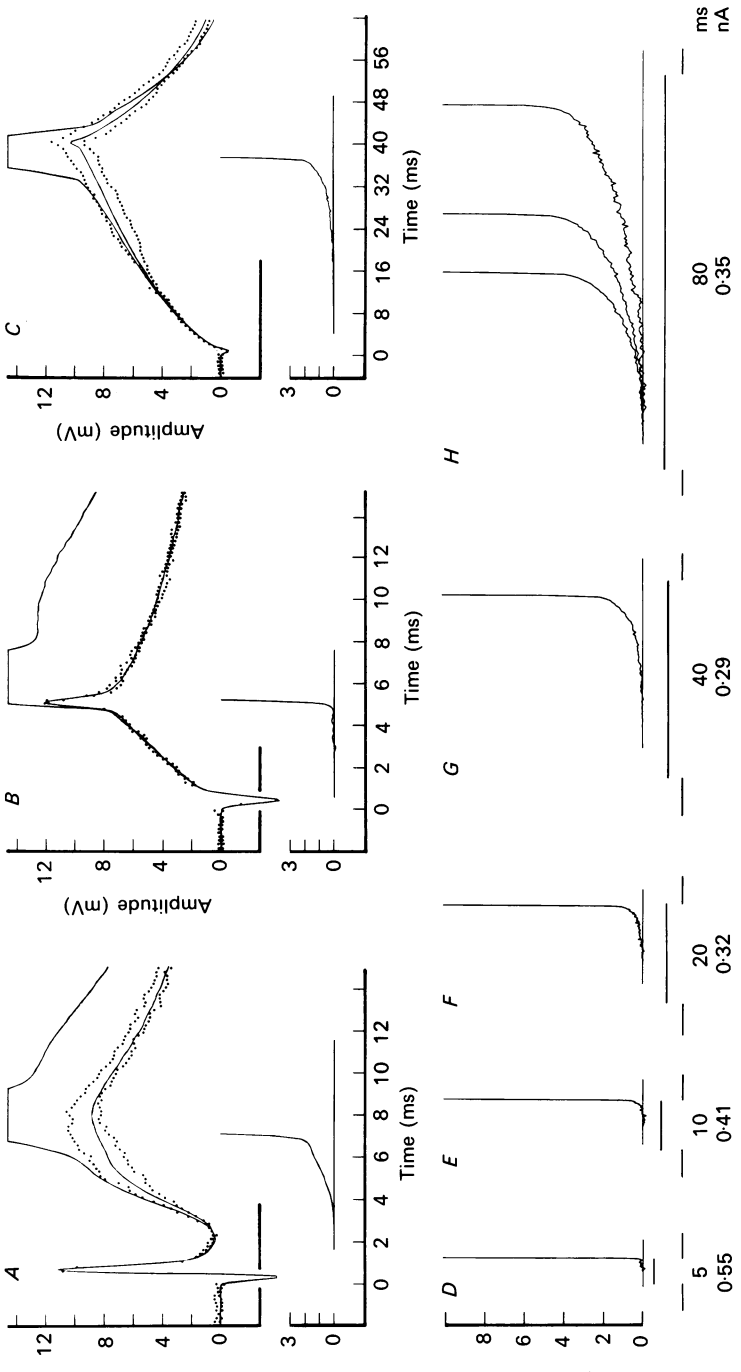

Fig. 10. Comparison of SyPP and pulse-induced slow prepotential. *A*, the averaged traces of sixty action potentials and forty-one subthreshold EPSPs (continuous lines) from a CA1 cell in response to a constant stimulus strength. The dots indicate the largest and smallest subthreshold EPSP. The averaged subtraction record at the bottom shows a SyPP preceding the large amplitude action potential. *B*, the averaged traces of twenty-one spike-containing and twenty-seven spike-free responses from the same cell to depolarizing current pulses of 5 ms duration injected into the soma. Although the pulse-induced responses have a similar rise time as the EPSP, the averaged subtraction record at the bottom shows no prepotential in front of the action potential. *C*, the averaged traces of nineteen spike-containing and twenty-three spike-free responses of the same cell to 40 ms long depolarizing current pulses. The averaged subtraction record shows a prepotential with a slower time course than in *A* (note the different time scale). *D–H*, the averaged subtraction records from the same cell in response to 5, 10, 20, 40 and 80 ms long depolarizing current pulses, all giving a FP of around 0·5. Same time scale.

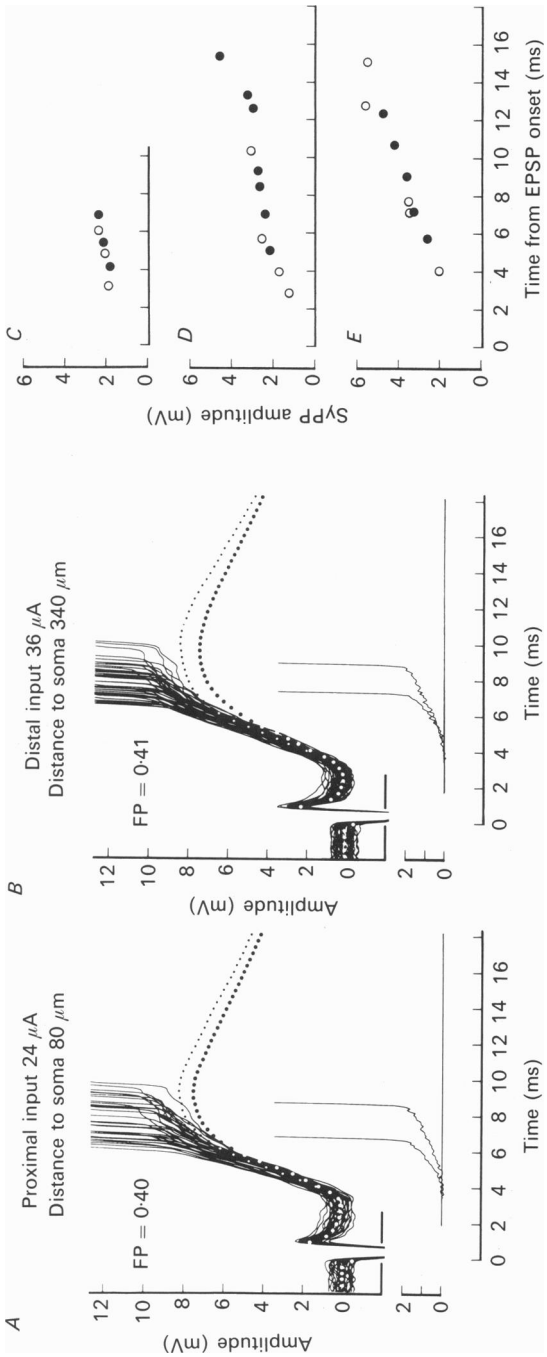

Fig. 11. SyPPs elicited by proximal and distal dendritic synaptic inputs. *A*, the CA1 pyramidal cell responded with thirty-five action potentials to 'proximal' stimuli of 24 μA through a stimulating electrode placed in stratum radiatum 80 μm from the soma. The mean of fifty-three subthreshold EPSPs and the mean of thirty-five subthreshold EPSPs selected for subtraction are drawn by the large and small dots, respectively. *B*, as *A*, but responses of the same cell (forty-five action potentials and sixty-four subthreshold EPSPs) to 'distal' stimuli of 36 μA, delivered through another stratum radiatum-stimulating electrode, 340 μm from the soma. *C–E*, the SyPP amplitude to proximal (○) and distal inputs (●) plotted against the time from the EPSP onset in three selected cells which showed a similar FP to both inputs (difference less than 5%).

(small dots) both have a slightly steeper rising phase in the proximal responses (*A*) than in the distal ones (*B*). In contrast, the SyPPs elicited by the two inputs show no apparent difference, even when adjusting for the slight latency variation of the large amplitude action potentials.

A further comparison of the SyPPs to proximal and distal inputs from three cells is presented in Fig. 11*C–E*. The open and filled circles represent the SyPP amplitudes plotted with reference to the EPSP onset. All cells showed a similar distribution of the SyPP amplitude *versus* spike latency for both inputs. In conclusion, the SyPPs elicited by FP-matched proximal and distal synaptic stimulation are nearly identical.

DISCUSSION

Existence of synaptic prepotentials

Because action potentials were elicited only from the largest of a group of EPSPs at a constant stimulus strength, one could ask whether the described SyPPs are not just examples of particularly large amplitude EPSPs. The distinction between SyPPs and the underlying EPSP rests on five sets of observations. (i) Shape difference: all SyPPs are upwards concave while the relevant parts of subthreshold EPSPs are upwards convex. (ii) Coupling to the action potential: the SyPPs are locked in time to the action potentials (most clearly for the long latency examples), and not to a particular phase of the EPSP. Some SyPPs may even start after the summit of the EPSP. (iii) Pulse interference: a hyperpolarizing pulse may delay or totally block the large amplitude action potential and unmask a deflection that could be an underlying SyPP. (iv) Depolarization effect: depolarization of the cell gives an enhancement of the SyPP, but a reduction of the EPSP amplitude. (v) Pharmacological modulation: intracellular injection of QX-314 may abolish the SyPP with preserved amplitude of the EPSP and the large amplitude action potential. APV reduced the EPSP, but did not affect the SyPP.

The present description of SyPPs resembles that given by Eccles and his collaborators for synaptically activated action potential in cat motoneurones (Coombs *et al.* 1955). They noted the difficulty of establishing a precise voltage threshold for the action potential. Because the EPSP/spike transition was not abrupt, they used the point of maximum upward curvature at the spike onset as an index of the threshold, but admitted that this point was not a true indication of the critical potential for generating the spike, because a 'depolarizing creep' of potential preceded it. We suggest that this 'creep' of potential is probably a SyPP. The slightly longer duration of the hippocampal SyPPs may be due to the longer rise time of the EPSPs as compared to motoneurones, allowing the process more time to develop.

The SyPP is clearly different from the fast prepotential of hippocampal neurones (Spencer & Kandel, 1961) in having a slower time course and often being present on all spike-containing traces in a cell. The SyPP also differs from a local nerve response, both in its duration and in its form (Hodgkin, 1939), although its function may be similar.

Validity of the subtraction procedure for isolating the synaptic prepotential

Both the amplitude and the time course of the SyPP depends upon the selection of a correct subthreshold EPSP for subtraction. Unlike other threshold events it was not sufficient to compare the traces with and without action potentials. The main reason was the variability of the EPSP amplitude at spike threshold, in spite of a constant stimulus strength. Thus, for each spike-eliciting EPSP we had to select a spike-free EPSP with a closely similar rising phase trajectory. Because all EPSPs had the same shape (Fig. 3*A*), the initial part could be used to predict the rest of the EPSP. Because the amplitude of the SyPP was found to be nearly similar for certain defined lengths of the chosen template (Fig. 4*C*), the reported amplitude value appears as an acceptable index for the process. Unfortunately, the slope measurements are less certain. Further, it is not possible to give a definite onset time or a specific voltage threshold for the SyPP due to its gradual start and to the inherent uncertainty in selecting a template for subtraction. The upward concave shape of the SyPP is not due to the averaging technique since it was also found for individual traces and for averages of spikes with nearly identical latencies. Neither is it due to the subjective choice of the template length for selecting EPSPs for subtraction, because the shape of the SyPP remained for all tested durations of the template (Fig. 4*B*).

The coupling to the following action potential appeared self-evident for spikes with long latency. However, whether the shortest latency spikes were also preceded by a SyPP could not be decided by eye, but required subtraction of the subthreshold EPSP component from the full response.

Nature of the process giving rise to the synaptic prepotential

The SyPP has certain features in common with the slow prepotentials which precede action potentials induced by depolarizing current pulses injected into the soma (Lanthorn, Storm & Andersen, 1984; Storm & Hvalby, 1985). This prepotential type is sensitive to tetrodotoxin and QX-314, but not affected by calcium channel blockers (Storm, 1984; MacVicar, 1985; Hu, 1991). Because the SyPP can be blocked by intracellular QX-314 at a dose which is below or at the spike-blocking concentration, a sodium current is probably involved. A possible candidate is the persistent sodium current observed in cat sensorimotor cortical neurones (Stafstrom, Schwindt & Crill, 1982; Stafstrom *et al.* 1985), in hippocampal pyramidal cells (French & Gage, 1985) and in cerebellar Purkinje cells (Llinás & Sugimori, 1980), which may be related to the threshold channels found in squid axons (Gilly & Armstrong, 1984). At the single-channel level a non-inactivating sodium current has been identified in cultured hippocampal neurones (Masukawa, Hansen & Shepherd, 1991). The just-subthreshold, non-inactivating current, proposed by Hotson, Prince & Schwartzkroin (1979) to be responsible for anomalous rectification in CA1 cells, was blocked *both* by calcium and sodium channel blockers. Therefore, it appears to be different from the process underlying the SyPP. Alternatively, the situation may be similar to cardiac and skeletal muscle where a slow sodium current has been attributed to multiple re-openings of single classical sodium channels (Patlak & Ortiz, 1985, 1986; Nilius, 1988; Josephson & Sperelakis, 1989). A third alternative

is a process similar to the 'window' current of cardiac Purkinje fibres. The latter is seen as the steady-state component of the fast sodium current, resulting from the crossover of the activation and inactivation curves which control the opening of sodium channels (Attwell, Cohen, Eisner, Ohba & Ojeda, 1979). The problem can only be solved by experiments with adequate clamping of the SyPP-generating membrane.

Other synaptically triggered voltage-sensitive currents could conceivably play an additive role. In motoneurones, a voltage-dependent EPSP enhancement follows injection of tetraethylammonium ions (Clements, Nelson & Redman, 1986). Unlike the SyPP, however, this process did neither show exponential growth nor a close association with the action potential. A major contribution of the A- or the D-current also appears unlikely, because of the different activation levels, time constants and responses to depolarization (Storm, 1990). Finally, the SyPP does not appear to be a NMDA receptor-mediated component of the EPSP, since it was not affected by APV application.

Possible generation site of synaptic prepotentials

The inability of a 5 ms depolarizing pulse to induce a prepotential is in striking contrast to the efficiency of the EPSP, showing the same rise time, suggesting that the soma normally does not produce prepotentials. Nor do the SyPPs seem to be generated near the initial axon since the somatic current injection should have better access to this site than the excitatory synaptic current. Furthermore, antidromic action potentials never started with a prepotential. Therefore, the ease with which the EPSP elicits the SyPP suggests that the site of prepotential generation is in the dendritic tree. It is compatible with the finding of Na^+-mediated active responsiveness in the dendrites (Wong, Prince & Basbaum, 1979; Masukawa *et al.* 1991). The problem may be resolved if a method for locating the binding sites for intracellularly injected QX-314 could be developed.

Long pulses will charge a greater part of the dendritic tree than the short pulses can, thus probably reaching the prepotential threshold at the proposed dendritic site of generation. The prepotential is then conducted electrotonically to the recording electrode in the soma. The ability of distal synapses to create SyPPs with the same ease as more proximally located inputs further suggests that such sites of generation could be distributed in several parts of the dendritic tree.

Possible physiological role of synaptic prepotentials

Our findings lead us to propose that a just-suprathreshold EPSP triggers a two-phased action potential. The SyPP is seen as an initial process which in turn triggers a fast, large amplitude action potential with a high safety factor. Alternatively, the SyPP could represent a protracted start of a single action potential process. Against this interpretation stands the abrupt slope change at the transition from the SyPP to the spike, and the selective blockade of SyPP by QX-314 injection, as well as the unmasking of an isolated SyPP when the large amplitude action potential is blocked by a hyperpolarizing pulse.

With its all-or-none appearance and very tight coupling to the large amplitude action potential, the SyPP appears as a regenerative process somewhat similar to the

regenerative dendritic potentials seen in Purkinje cells in response to synaptic activation (Chan, Hounsgaard & Midtgaard, 1989). Such a pacemaker-like process could be particularly important for cells with distributed dendritic synapses. Its presence may explain much of the large fluctuations of spike latency in spite of a constant stimulus strength, due to the variation of the duration and amplitude of the SyPP.

The SyPP appears to add itself to near-threshold EPSPs to bring the cell to discharge. Thus, it might be seen as a facilitory process for weak excitatory synaptic activity when the cell is close to the firing level. It would contribute most during such conditions, for example under cholinergic influence during behavioural arousal (Dodd, Dingledine & Kelly, 1981; Benardo & Prince, 1982). Under these circumstances, the long-lasting cellular depolarization would tend to inactivate fast sodium channels and thereby increase the threshold for large amplitude action potentials. The prepotential mechanism will counteract the increased threshold, thus improving the safety factor for spike initiation. In contrast, at hyperpolarized levels, the SyPP would contribute less or nothing, so that a larger EPSP would be required to discharge the cell. The SyPP will also counteract processes mediated by the transient A- and D-currents (Gustafsson, Galvan, Grafe & Wigström, 1982; Storm, 1988) and the M-current (Halliwell & Adams, 1982) and inhibitory processes which all tend to bring the cell to a more hyperpolarized level.

If the SyPP is developed to a different degree in different areas of the dendrite, it could compensate synapses otherwise in a disadvantageous situation. Since the synaptic barrage may well differ in different parts of the dendritic tree, the SyPP process might be a way to enhance a local depolarization at the expense of more distributed inputs to the dendritic tree. Since some processes, particularly those in which synaptic plasticity is involved, depend upon the degree of dendritic depolarization, it could also promote the condition necessary for long-term potentiation to occur (Wigström, Gustafsson, Huang & Abraham, 1986; Hvalby, Lacaille, Hu & Andersen, 1987).

This work was supported by the Norwegian Research Council for Science and the Humanities (grant 326.88/007), Anders Jahres Fond, and by a NORAD Fellowship (G.-Y.H.) from the Norwegian Ministry for Development and by a NATO Science Fellowship (J.-C.L.) from the Natural Sciences and Engineering Research Council of Canada. We are grateful to J. Storm for instructive discussions and valuable comments on the manuscript, and to T. Reppen, P. Skjeflo, K. Buday and A. Byrkjeland for technical assistance.

REFERENCES

ANDERSEN, P., LACAILLE, J.-C., HVALBY, Ø., HU, G.-Y., PIERCEY, B. W. & ØSTBERG, T. (1986). Synaptic prepotentials – an intermediary process in synaptic excitation. *Acta Physiologica Scandinavica* **128**, 17A.

ANDERSEN, P., SILFVENIUS, H., SUNDBERG, S. H. & SVEEN, O. (1980). A comparison of distal and proximal dendritic synapses on CA1 pyramids in guinea-pig hippocampal slices *in vitro*. *Journal of Physiology* **307**, 273–299.

ANDERSEN, P., STORM, J. & WHEAL, H. V. (1987). Thresholds of action potentials evoked by synapses on the dendrites of pyramidal cells in the rat hippocampus *in vitro*. *Journal of Physiology* **383**, 509–526.

ANDREASEN, M., LAMBERT, J. D. C. & JENSEN, M. S. (1989). Effects of new non-*N*-methyl-D-

aspartate antagonists on synaptic transmission in the *in vitro* rat hippocampus. *Journal of Physiology* **414**, 317–336.

ATTWELL, D., COHEN, I., EISNER, D., OHBA, M. & OJEDA, C. (1979). The steady state TTX-sensitive ('window') sodium current in cardiac Purkinje fibres. *Pflügers Archiv* **379**, 137–142.

BENARDO, L. S. & PRINCE, D. A. (1982). Cholinergic excitation of mammalian hippocampal pyramidal cells. *Brain Research* **249**, 315–331.

CHAN, C. Y., HOUNSGAARD, J. & MIDTGAARD, J. (1989). Excitatory synaptic responses in turtle cerebellar Purkinje cells. *Journal of Physiology* **409**, 143–156.

CLEMENTS, J. D., NELSON, P. G. & REDMAN, S. J. (1986). Intracellular tetraethylammonium ions enhance group Ia excitatory post-synaptic potentials evoked in cat motoneurones. *Journal of Physiology* **377**, 267–282.

COOMBS, J. S., ECCLES, J. C. & FATT, P. (1955). Excitatory synaptic action in motoneurones. *Journal of Physiology* **130**, 374–395.

DODD, J., DINGLEDINE, R. & KELLY, J. S. (1981). The excitatory action of acetylcholine on hippocampal neurones of the guinea pig and rat maintained in vitro. *Brain Research* **207**, 109–127.

FETZ, E. E. & GUSTAFSSON, B. (1983). Relation between shapes of postsynaptic potentials and changes in firing probability of cat motoneurones. *Journal of Physiology* **341**, 387–410.

FRENCH, C. R. & GAGE, P. W. (1985). A threshold sodium current in pyramidal cells in rat hippocampus. *Neuroscience Letters* **56**, 289–293.

GILLY, W. F. & ARMSTRONG, C. M. (1984). Threshold channels – a novel type of sodium channel in squid giant axon. *Nature* **309**, 448–450.

GUSTAFSSON, B., GALVAN, M., GRAFE, P. & WIGSTRÖM, H. (1982). A transient outward current in a mammalian central neurone blocked by 4-aminopyridine. *Nature* **299**, 252–254.

HABLITZ, J. J. & LANGMOEN, I. A. (1986). *N*-Methyl-D-aspartate receptor antagonists reduce synaptic excitation in the hippocampus. *Journal of Neuroscience* **6**, 102–106.

HALLIWELL, J. V. & ADAMS, P. R. (1982). Voltage-clamp analysis of muscarinic excitation in hippocampal neurones. *Brain Research* **250**, 71–92.

HODGKIN, A. L. (1939). The subthreshold potentials in a crustacean nerve fibre. *Proceedings of the Royal Society* B **126**, 87–121.

HOTSON, J. R., PRINCE, D. A. & SCHWARTZKROIN, P. A. (1979). Anomalous inward rectification in hippocampal neurones. *Journal of Neurophysiology* **42**, 889–895.

HU, G.-Y. (1991). Effects of depolarization and QX-314 injection on slow prepotentials in rat hippocampal pyramidal neurones *in vitro*. *Acta Physiologica Scandinavica* **141**, 235–240.

HU, G.-Y., HVALBY, Ø., PIERCEY, B. & ANDERSEN, P. (1989). Hippocampal EPSPs trigger action potentials by way of synaptic prepotentials (SyPP). *European Journal of Neuroscience*, suppl. **2**, 186.

HVALBY, Ø., LACAILLE, J.-C., HU, G.-Y. & ANDERSEN, P. (1987). Postsynaptic long-term potentiation follows coupling of dendritic glutamate application and synaptic activation. *Experientia* **43**, 599–601.

JOSEPHSON, I. R. & SPERELAKIS, N. (1989). Tetrodotoxin differentially blocks peak and steady-state sodium channel currents in early embryonic chick ventricular myocytes. *Pflügers Archiv* **414**, 354–359.

KIRKWOOD, P. A. & SEARS, T. A. (1982). The effects of single afferent impulses on the probability of firing of external intercostal motoneurones in cat. *Journal of Physiology* **322**, 315–336.

KNOX, C. K. & POPPELE, R. E. (1977). Correlation analysis of stimulus-evoked changes in excitability of spontaneously firing neurons. *Journal of Neurophysiology* **40**, 616–625.

LANTHORN, T., STORM, J. & ANDERSEN, P. (1984). Current-to-frequency transduction in CA1 hippocampal pyramidal cells: slow prepotentials dominate the primary range firing. *Experimental Brain Research* **53**, 431–443.

LLINÁS, R. & SUGIMORI, M. (1980). Electrophysiological properties of *in vitro* Purkinje cell somata in mammalian cerebellar slices. *Journal of Physiology* **305**, 171–195.

MACVICAR, B. A. (1985). Depolarizing prepotentials are Na^+ dependent in CA1 pyramidal neurones. *Brain Research* **333**, 378–381.

MASUKAWA, L. M., HANSEN, A. J. & SHEPHERD, G. (1991). Distribution of single-channel conductances in cultured rat hippocampal neurones. *Cellular and Molecular Neurobiology* **11**, 231–243.

NILIUS, B. (1988). Modal gating behavior of cardiac sodium channels in cell-free membrane patches. *Biophysical Journal* **53**, 857–862.

ØSTBERG, T., HU, G.-Y., HVALBY, Ø., PIERCEY, B. & ANDERSEN, P. (1986). Blocking of synaptic prepotential by injection of QX-314 in hippocampal pyramidal cells. *Acta Physiologica Scandinavica* **128**, 18A.

PATLAK, J. B. & ORTIZ, M. (1985). Slow currents through single sodium channels of the adult rat heart. *Journal of General Physiology* **86**, 89–104.

PATLAK, J. B. & ORTIZ, M. (1986). Two modes of gating during late Na^+ channel currents in frog sartorius muscle. *Journal of General Physiology* **87**, 305–326.

PROVENCHER, S. W. (1976). A Fourier method for the analysis of exponential decay curves. *Biophysical Journal* **16**, 27–41.

SPENCER, W. A. & KANDEL, E. R. (1961). Electrophysiology of hippocampal neurons. IV. Fast prepotentials. *Journal of Neurophysiology* **24**, 272–285.

STAFSTROM, C. E., SCHWINDT, P. C., CHUBB, M. C. & CRILL, W. E. (1985). Properties of persistent sodium conductance and calcium conductance of layer V neurons from cat sensorimotor cortex in vitro. *Journal of Neurophysiology* **53**, 153–170.

STAFSTROM, C. E., SCHWINDT, P. C. & CRILL, W. E. (1982). Negative slope conductance due to a persistent subthreshold sodium current in cat neocortical neurons *in vitro*. *Brain Research* **236**, 221–226.

STORM, J. (1984). Two components of slow prepotentials in CA1 hippocampal pyramidal cells. *Acta Physiologica Scandinavica* **120**, 22A.

STORM, J. F. (1988). Temporal integration by a slowly inactivating K^+ current in hippocampal neurons. *Nature* **336**, 379–381.

STORM, J. F. (1990). Potassium currents in hippocampal pyramidal cells. *Progress in Brain Research* **83**, 161–187.

STORM, J. & HVALBY, Ø. (1985). Repetitive firing of CA1 hippocampal pyramidal cells elicited by dendritic glutamate: slow prepotentials and burst–pause pattern. *Experimental Brain Research* **60**, 10–18.

WIGSTRÖM, H., GUSTAFSSON, B., HUANG, Y.-Y. & ABRAHAM, W. C. (1986). Hippocampal long-term potentiation is induced by pairing single afferent volleys with intracellular injected depolarizing current pulses. *Acta Physiologica Scandinavica* **126**, 317–319.

WONG, R. K. S., PRINCE, D. A. & BASBAUM, A. I. (1979). Intradendritic recordings from hippocampal neurons. *Proceedings of the National Academy of Sciences of the USA* **76**, 986–990.